

1
2 **KINETIC MODELLING AND PERFORMANCE PREDICTION OF A HYBRID**
3 **ANAEROBIC BAFFLED REACTOR TREATING SYNTHETIC**
4 **WASTEWATER AT MESOPHILIC TEMPERATURE**

5

6 **S. Ghaniyari-Benis^a, A. Martín^b & R. Borja^c ***

7

8 ^a Department of Chemical and Petroleum Engineering, Sharif University of Technology
9 (SUT), P.O. Box 11365-8639, Tehran, Iran.

10 ^b Departamento de Química Inorgánica e Ingeniería Química, Facultad de Ciencias,
11 Campus Universitario de Rabanales, Edificio C-3, Ctra. Madrid-Cádiz, Km 396, 14071-
12 Córdoba, Spain.

13 ^c Instituto de la Grasa (C.S.I.C.), Avda. Padre García Tejero, 4, 41012-Sevilla, Spain.

14

15 * Corresponding author: R. Borja (Tel.: +34 95 4689654; fax: +34 95 4691262; E-mail
16 address: rborja@cica.es (R. Borja).

17

18

19 **Abstract**

20 A modelling study on the anaerobic digestion process of a synthetic medium-
21 strength wastewater containing molasses as a carbon source was carried out at different
22 influent conditions. The digestion was conducted in a laboratory-scale hybrid anaerobic
23 baffled reactor with three compartments and a working volume of 54 L, which operated
24 at mesophilic temperature (35 °C). Two different kinetic models (one model was based
25 on completely stirred tank reactors (CSTR) in series and the other an axial diffusion or
26 dispersion model typical of deviations of plug-flow reactors), were assessed and

27 compared to simulate the organic matter removal or fractional conversion. The kinetic
28 constant (k) obtained by using the CSTR in series model was $0.60 \pm 0.07 \text{ h}^{-1}$, while the
29 kinetic parameter achieved with the dispersion model was $0.67 \pm 0.06 \text{ h}^{-1}$, the dispersion
30 coefficient (D) being 46. The flow pattern observed in the reactor studied was
31 intermediate between plug-flow and CSTR in series systems, although the plug-flow
32 system was somewhat predominant. The dispersion model allowed for a better fit of the
33 experimental results of fractional conversions with deviations lower than 8% between
34 the experimental and theoretical values. By contrast, the CSTR in series model
35 predicted the behaviour of the reactor somewhat less accurately showing deviations
36 lower than 10% between the experimental and theoretical values of the fractional
37 conversion.

38

39 *Keywords:* Modelling; hybrid anaerobic baffled reactor; synthetic wastewater; CSTR in
40 series model; dispersion model.

41

42 **1. Introduction**

43

44 In recent years, anaerobic technology has been applied to the treatment of many
45 medium and high-strength industrial wastewaters. Taking into account the slow growth
46 of many anaerobic microorganisms, particularly methanogenics, the main objectives of
47 the efficient reactor design should be high retention time of bacterial cells with very
48 little loss of microorganisms from the bioreactor [1, 2]. The technological challenge to
49 improve anaerobic digestion lies in enhancing bacterial activity together with good
50 mixing to ensure adequate contact between the cells and their substrate [3, 4].

51 The anaerobic baffled reactor (ABR) consists of a cascade of baffled
52 compartments where the wastewater flows upward through a bed of anaerobic sludge
53 after being transported to the bottom of the compartment. The ABR does not require the
54 sludge to granulate in order to perform effectively, although granulation can occur over
55 time [5, 6]. Experiments with lab-scale reactors have shown that the ABR is very stable
56 under shock loads due to its compartmentalised structure [6, 7, 8]. In addition, the ABR
57 has many potential advantages, i.e. no requirement of biomass with unusual settling
58 properties and low capital and operating costs coupled with mechanical simplicity [6].

59 In the present study, a hybrid anaerobic baffled (HABR) reactor or multistage
60 biofilm reactor with three compartments was used. This reactor configuration can be
61 considered as a combination of the anaerobic baffled reactor (ABR) and upflow
62 anaerobic fixed bed (UAFB) system which include the advantages of the ABR systems
63 and anaerobic filters. These properties are: better resilience to hydraulic and organic
64 shock loadings, longer biomass retention times; lower sludge yields, and the ability to
65 partially separate between the various phases of anaerobic catabolism [6, 9]. The latter
66 causes a shift in bacterial population allowing increased protection against toxic
67 materials and higher resistance to changes in environmental parameters such as pH and
68 temperature. The greatest advantage of this reactor configuration is probably its ability
69 to separate acidogenesis and methanogenesis longitudinally down the reactor, allowing
70 the reactor to behave as a two-phase system without the associated control problems and
71 high costs.

72 Kinetic studies are helpful for reproducing the empirical behaviour of the
73 anaerobic process and understanding the metabolic routes of biodegradation, while
74 simultaneously saving time and money [10]. However, the development of an up-to-

75 date model of organic matter anaerobic degradation is complex with considerable
76 difficulties due to the high number of variables affecting the anaerobic system [11, 12].

77 A model was developed for the anaerobic digestion of a glucose-based medium in
78 an innovative high-rate reactor known as the periodic anaerobic baffled reactor (PABR).
79 In this model, each compartment is considered as two variable volume interacting
80 sections, with constant total volume, one compartment with high solids and the other
81 one with low solid concentrations, with the gas and liquid flows influencing the material
82 flows between the two sections. For the simulation of glucose degradation, the biomass
83 was divided into acidogenic, acetogenic and methanogenic groups of microorganisms.
84 The model succeeded in predicting the reactor performance as the organic loading rate
85 was gradually increased [13]. Another kinetic model for predicting the behaviour of the
86 PABR was developed based on batch experiments using glucose as substrate [5]. The
87 PABR may be operated as an upflow anaerobic sludge blanket (UASB) reactor, an ABR
88 or at an intermediate mode. The key assumption of this model was that the hydraulic
89 behaviour of a PABR was equivalent to the behaviour of CSTRs in series as regards the
90 dissolved matter. The model adequately predicted the experimental behaviour of this
91 glucose-fed PABR and was also used to examine the performance of this reactor as a
92 function of the operating conditions, both for constant and varying loading rates. It was
93 shown that the reactor would best be operated as a UASB or an ABR [5].

94 Another kinetic model was recently developed for explaining the performance of a
95 four-compartment ABR, incorporating granular sludge biomass and operating at
96 different hydraulic retention times (HRT) in the range of 3 to 24 hours using dilute
97 aircraft de-icing fluid with total chemical oxygen demand (COD) concentrations in the
98 range of 300-750 mg/L. However, the first-order empirical model initially developed for
99 describing the reactor performance did not adequately predict the total COD removal

100 efficiency in the reactor with unsatisfactory results between the experimental and
101 theoretical values [14].

102 A mathematical model of the baffled reactor performance was developed and
103 applied using a concept of completely mixed reactors operating in series to describe the
104 performance of a modified laboratory-scale (150 L) ABR using molasses wastewater as
105 substrate [15]. This reactor had three chambers and a final settler. The first two
106 compartments each had a 10 cm layer of plastic media (Pall rings with a specific surface
107 area of $142 \text{ m}^2/\text{m}^3$) near the liquid surface. The third chamber had the upper half filled
108 with a modular corrugated block. This kinetic analysis focussed on the granular sludge
109 bed, with total mass of granular sludge as the main parameter. The model results were
110 in good agreement with the experimental data [15].

111 However, despite the advantages offered by the hybrid anaerobic baffled reactors
112 few mathematical analyses have been reported to date for modelling the kinetic
113 behaviour of these reactors and for simulating the variation of the total COD removal
114 efficiency under several operating conditions. Therefore, the main objective of this
115 work was to compare two different kinetic models: a model based on the concept of
116 completely stirred tank reactors (CSTR) in series and an axial diffusion or dispersion
117 model, typical of deviations of plug-flow reactors, in the anaerobic treatment of
118 synthetic wastewater containing molasses as a carbon source. These mathematical
119 models have not been reported up to now in the literature to describe the kinetic
120 performance of this specific type of hybrid reactor operating under varying HRTs,
121 organic loading rates and influent substrate concentrations. The anaerobic hybrid reactor
122 used was composed of three sequential compartments, where each one formed a packed
123 bed using Pall rings (PVC) as a medium for supporting the biofilm formation.

124

125

126 **2. Materials and methods**

127

128 *2.1. Experimental set-up*

129

130 The hybrid anaerobic baffled reactor was composed of three sequential
131 compartments, which were fabricated from Plexiglas. The reactor dimensions were 58
132 cm long, 24 cm wide and 44 cm high, with a total working volume of 54 L. The
133 wastewater had an upflow mode inside each stage. The baffle spacing was determined
134 by keeping the compartments the same size, the ratio between the up-corner and down-
135 corner being 4:1. The height and width of baffles were 38 and 6 cm respectively. The
136 baffles inside the reactor were used to direct the flow of wastewater in an upflow mode
137 through a series of compartments where each one formed a packed bed using Pall Rings
138 as a media for supporting the biofilm formation. The main characteristics of Pall Rings
139 as a microorganism support medium were: material, PVC; nominal size, 25 mm; height,
140 25 mm; thickness, 1 mm; surface area, 206 m²/m³; and 90% porosity. This kind of
141 packing resulted in increased process efficiency and a decrease in clogging as reported
142 in previous works [16]. A diagram of the hybrid anaerobic baffled reactor used is given
143 in Figure 1.

144 The initial porosity of the beds was 77% and after the immobilization of anaerobic
145 cells they had a similar porosity (65%). Each compartment of the reactor was filled up
146 to 64% of its active volume with the pall packing and equipped with sampling ports that
147 allowed liquid samples to be withdrawn. A peristaltic pump (model “Omega”,
148 FPUDVS2000 Series) was used to feed the bioreactor. The reactor was covered with a
149 water jacket keeping the operational temperature at 35°C ± 0.5 °C.

150

151 2.2. *Synthetic wastewater*

152 The reactor was fed with synthetic wastewater containing molasses as a carbon
153 source. Synthetic wastewater was used in the present work with the aim of avoiding and
154 minimising variations in wastewater composition between experiments. In addition, real
155 wastewater with the same characteristics is not always available to be used in the
156 laboratory. A fresh batch was made every day by diluting molasses with tap water to
157 achieve the total COD concentration required for each loading rate. The characteristics
158 of the molasses used were (mean values \pm standard deviations) : pH, 7.6 ± 0.3 ; COD
159 (total COD throughout the paper), 1124 ± 35 mg/L; BOD₅: 411 ± 12 mg/L; Kjeldahl
160 nitrogen, 16.6 ± 0.5 mg/L; total phosphate, 0 mg/L; Ca²⁺, 59.2 ± 1.8 mg/L; K⁺, 3.1 ± 0.1
161 mg/L; alkalinity, 196 ± 6 mg/L; total sugars, $47.4\pm 1.5\%$; free sugars, $18.7\pm 0.6\%$; non-
162 fermentable sugars, $6.0\pm 0.2\%$; total dissolved solids (TDS), $38\pm 1\%$. These values
163 summarize the main features of the molasses obtained by diluting 1 g of raw molasses
164 into 1 L of distilled water. The COD:N ratio of the wastewater used was 67:1. Only
165 during the start-up period were urea and ammonium phosphate used as sources of
166 nitrogen and phosphorus, respectively. A total dose of 925 mL of a micronutrient and
167 trace metal solution was added only at the beginning of the start-up period of the
168 reactor. The composition of this micronutrient and trace metal solution was:
169 CoCl₂·6H₂O, 0.25 mg/L; H₃BO₃, 0.05 mg/L; FeCl₂·2H₂O, 2 mg/L; MnCl₂·4H₂O, 0.5
170 mg/L; ZnCl₂, 0.05 mg/L; CuCl₂, 0.15 mg/L; Na₂MoO₄·2H₂O, 0.01 mg/L; NiCl₂·6H₂O,
171 0.01 mg/L; Na₂SeO₃, 0.01 mg/L; AlCl₃·6H₂O, 0.05 mg/L; MgCl₂, 1 mg/L;
172 MgSO₄·7H₂O, 0.3 mg/L; CaCl₂·2H₂O, 0.18 mg/L [9]. These nutritious substances were
173 used to favour the growth of the biofilm on the surface media. During the start-up
174 period, COD:N:P ratio was 100:5:1. When a steady-state condition was achieved, the
175 COD:N:P ratio changed to 350:5:1. In order to prevent the build-up of a localized acid

176 zone in the reactor, sodium bicarbonate was used for supplementing the alkalinity.
177 NaHCO_3 is the only chemical which gently shifts the equilibrium to the desired value
178 without disturbing the physical and chemical balance of the sensitive microbial
179 population [17].

180

181 *2.3. Reactor inoculum*

182 The microorganisms used as inoculum in the reactor originated from the sludge of
183 the ABR system treating non-alcoholic beer wastewater of the Berinuscher Company
184 located in Shiraz, Iran. The basic characteristics of the anaerobic inoculum used were
185 (mean values \pm standard deviations): total acidity, 178 ± 6 g acetic acid/ m^3 ; total solid
186 content, 69.5 ± 2.1 kg/ m^3 ; volatile solid content, 28.3 ± 0.3 kg/ m^3 ; bicarbonate alkalinity,
187 1374 ± 45 g CaCO_3/m^3 ; and pH, 7.3 ± 0.3 . A total volume of 19 L of the above-mentioned
188 inoculum was added to the reactor and distributed among compartments before starting
189 the experiments.

190

191 *2.4. Experimental procedure*

192 At the beginning of the start-up, the reactor was run in a batch mode. During this
193 time, sludge was acclimated to the synthetic wastewater by using influent COD
194 concentrations in the range of 0.5 to 1.5 g/L. This initial period lasted 45 days. The
195 continuous operation of the system was started using an initial COD concentration of
196 3000 mg/L at a HRT of 2 days, which was equivalent to an organic loading rate (OLR)
197 of 1.5 kg COD/ m^3 d. A COD removal efficiency of 70% was achieved at this level.
198 When there was no fluctuation in different parameters such as COD and volatile fatty
199 acids (VFA) in each compartment, then the OLR increased to 3 kg COD/ m^3 d (HRT = 1
200 day) as the input flow-rate increased. The reactor was operated at this OLR for 45 days.

201 A COD removal efficiency of 91.6% was achieved at this OLR. An alkalinity value of
202 900 mg/L in the form of CaCO₃ was added at this stage. COD removal profile and pH
203 variations trend were monitored during this period. It was observed that the COD
204 decreased from 980 to 540 mg/L, from 710 to 340 mg/L and from 460 to 250 mg/L in
205 the compartments 1, 2 and 3, respectively. As could also be observed, there were some
206 irregularities in the pH value variations during the first few days, but as time went by
207 microbial selection and zoning were encouraged inside the reactor, with the
208 acidogenesis in compartments closer to the inlet. Specifically, pH values ranged
209 between 6.5–6.8, 6.4–7.3 and 6.5–7.6 in compartments 1, 2 and 3, respectively, during
210 this start-up period (45 days).

211 Two sets of experiments were carried out. A first group of experiments was
212 performed to study the influence of reducing the HRT on the system performance. The
213 reactor was fed with diluted molasses containing 3000 mg COD/L at two different
214 HRTs of 16 h and 8 h, which were equivalent to OLRs of 4.5 and 9 kg COD/m³ d. The
215 COD and volatile fatty acid (VFA) concentration changes in all compartments and
216 reactor effluents were monitored.

217 In the second part of the experiments, the effect of different OLRs was studied by
218 varying the COD of the influent substrate at a constant retention time. Specifically, the
219 reactor was fed with diluted molasses containing 3000, 4500 and 6000 mg COD/L at a
220 constant HRT of 16 h. The amount of COD eliminated and VFA concentration
221 changing profiles were obtained. All samples were analysed in triplicate and the final
222 results expressed as means.

223 The operating conditions studied for the two sets of experiments carried out were
224 selected taking into account the operational conditions evaluated previously in other
225 ABRs treating different wastewaters.

226

227 *2.5. Analytical methods*

228 The total COD concentration was measured by using a semi-micro method [18].
229 Alkalinity was determined in accordance with the standard method 2320 B of APHA
230 [19]. The concentration of VFA was determined by using HPLC according to Björnsson
231 et al. [20]. Total and volatile solids were determined according to the method number
232 2540 B [19]. The pH was determined with a Crison, model basic 20 pH-meter.
233 Phosphate was measured by spectrophotometry (880 nm) using the normalized method
234 4500 P [19]. Kjeldahl nitrogen was determined according to the standard method
235 number 4500-B [19]. Finally, Ca^{2+} and K^{+} were measured by atomic absorption
236 spectrophotometry.

237

238 *2.6. Software used*

239 SigmaPlot software (version 9.0) was used to elaborate all the graphs and Figures
240 of this study and to perform the statistical analyses. Mathcad software (version 14) was
241 used to solve the mathematical equations corresponding to the two models assessed.

242

243

244 **3. Results and Discussion**

245

246 *3.1. Operational behaviour of the HABR*

247 A previous study reported the operational performance of the HABR under
248 different experimental conditions [9]. Specifically, during the start-up period (first 45
249 days of operation), pH fluctuations were observed because there was no microbial
250 selection or zoning, but as the experiments progressed, results showed that phase

251 separation had occurred inside the reactor. COD removal percentages of 91.5%, 91.5%,
252 90.0% and 88.3% were achieved at organic loading rates of 3.0, 4.5, 6.75 and 9.0 kg
253 COD/m³ day, respectively. A decrease in HRT from 24 h to 16 h had no effect on COD
254 removal efficiency. When HRT decreased to 8 h, COD removal efficiency was still
255 84.7%. The VFA/alkalinity ratio can be used as a measure of process stability [20]:
256 when this ratio is less than 0.3-0.4 (equiv. acetic acid/equiv. CaCO₃) the process is
257 considered to be operating favourably without acidification risk. As could be observed
258 the ratio values were lower than the suggested limit value for all HRTs and OLRs
259 studied in the present work, showing the high stability of this reactor for all the
260 operating conditions assessed. Recirculation ratios of 0.5 and 1.0 had no effect on COD
261 removal but other factors such as the volatile fatty acid (VFA) content were affected.
262 The effect of toxic shock was also investigated and results showed that the main
263 advantage of using this bioreactor lies in its compartmentalized structure [9].

264

265 3.2. *Mathematical modelling*

266 The fractional conversion or organic matter removal efficiency (per one) can be
267 defined as the ratio between the amount of COD eliminated and the COD fed [21].
268 Figures 2 and 3 show the variation of the fractional conversion in the three
269 compartments of the HABR for the first set of experiments corresponding to HRTs of
270 16 h and 8 h respectively, and a constant influent substrate concentration (S_0) of 3000
271 mg COD/L. As can be seen in Figure 2, the steady-state fractional conversion or
272 removal efficiency (per one) increased from 0.788 to 0.872 and to 0.917 for the
273 compartments 1, 2 and 3 of the reactor during the assay corresponding to a HRT of 16 h
274 ($S_0 = 3000$ mg/L). A small decrease in the fractional conversion was observed when the
275 HRT decreased to 8 h (Figure 3). To be specific, the values of the conversion were

276 0.734, 0.795 and 0.847 for compartments 1, 2 and 3 of the reactor, respectively.
277 Therefore, a decrease in the final conversion of around 7% was observed when the HRT
278 dropped from 16 h to 8 h.

279 Figure 4 illustrates the effect of the influent substrate concentration ($S_0 = 3000$,
280 4500 and 6000 mg/L) on the fractional conversion for the three compartments of the
281 reactor when this operated at a constant HRT of 16 h. For the S_0 values of 3000, 4500
282 and 6000 mg COD/L, the steady fractional conversions for compartments 1 and 3
283 ranged between 0.818 and 0.918, 0.777 and 0.899 and 0.699 and 0.885, respectively.
284 Therefore a decrease in the conversion of only 3% was appreciated when the influent
285 substrate concentration doubled from 3000 to 6000 mg COD/L, which demonstrated
286 how effective this reactor configuration was against medium and high-strength
287 wastewaters.

288 In order to predict the fractional conversion or organic matter removal efficiency
289 (per one) for HABR, two different models were assessed and compared: a completely
290 stirred tank reactor (CSTR) in series model and an axial diffusion or dispersion model,
291 typically used for deviations of plug-flow systems.

292 When a stream of material flows steadily through a reactor or tank, where it takes
293 part in some process such as chemical or biological reaction, or simple mixing, it is
294 usual to make use of one of the following assumptions for the purpose of calculation
295 [22]:

- 296 a) The fluid in the tank is completely mixed, so that its properties are
297 uniform and identical with those of the outgoing stream. This assumption
298 is frequently made as the basis of calculation in stirred reactors.
- 299 b) Elements of fluid which enter the reactor at the same moment move
300 through it with constant and equal velocity on parallel paths, and leave at

301 the same moment. This type of behaviour is usually referred to as “piston
302 flow” or “plug flow” and is normally assumed when considering flow
303 through packed reactors, catalytic reactors, etc.

304 It is clear that there are many cases in which neither type of flow corresponds
305 exactly to the experimental facts [21-23]. It is of great importance to investigate the
306 discrepancies between the assumed and actual behaviour of these reactors, and where
307 necessary to allow for them in making kinetic calculations.

308 In the present study and given that the reactor used was a HABR with packing
309 medium in the three compartments, the hydrodynamic flow should be explained on the
310 basis of a plug flow model. The possible deviation of the behaviour of a plug-flow
311 model can be explained by the concurrence of two main factors: both liquid and gaseous
312 phases (biogas) circulate in the same direction and, in addition, due to the fact that the
313 upward velocity of the gas is much higher than the upward velocity of the liquid
314 (approximately 0.95 m/day), causing an airlift effect, which results in a mix of the liquid
315 phase and consequently in a deviation of the plug-flow hydrodynamic model. As a
316 consequence, either the CSTR in series model and the dispersion or axial diffusion
317 model are assayed and compared to predict the COD removal efficiency or fractional
318 conversion in the HABR.

319

320 *3.2.1. CSTR in series model*

321 This model assumes that the HABR is made up of three completely mixed tanks
322 with equal volume and connected in series. As was previously pointed out, the mix in
323 each tank is caused by the airlift effect generated by the produced biogas and circulation
324 of the liquid phase. Assuming that the steady-state conditions are achieved for each

325 reactor and that the substrate degradation follows a first-order kinetics, the following
326 COD balance can be set out:

$$327 \quad q \cdot S_{n-1} = q \cdot S_n + k \cdot S_n \cdot V \quad (1)$$

328 where: q is the volumetric flow-rate of the feed or influent; S_n is the COD in the
329 bioreactor or tank n ; S_0 is the influent or inlet COD; V is the bioreactor volume and k is
330 the kinetic constant of the process.

331 Defining the hydraulic retention time τ as the quotient: $\tau = V/q$ and the fractional
332 conversion (X) for any bioreactor (n) by the expression: $X_n = 1 - (S_n/S_0)$, the following
333 three equations can be established for a system with three CSTRs in series:

$$334 \quad X_1 = 1 - 1/(1 + k \cdot \tau) \quad (2)$$

$$335 \quad X_2 = 1 - 1/(1 + k \cdot \tau)^2 \quad (3)$$

$$336 \quad X_3 = 1 - 1/(1 + k \cdot \tau)^3 \quad (4)$$

337 The value of the kinetic constant, k , was determined from the experimental results
338 (Figures 2-4) by mathematical adjustment (non-linear regression) using Mathcad
339 software (version 14) based on the condition that the value of the sum of the squares of
340 the differences between the experimental and theoretical values should be at a
341 minimum. In this way, the value obtained for the kinetic constant, k , with its standard
342 deviation was $0.60 \pm 0.07 \text{ h}^{-1}$.

343 A CSTR in series model was also found to be applicable for studying the
344 hydrodynamic behaviour of a bench-scale horizontal flow anaerobic immobilized
345 sludge (HAIS) reactor filled with porous ceramic spheres (5 mm diameter). This reactor
346 operated at HRTs in the range of 2-7 hours using tracers with different characteristics
347 (bromophenol blue, dextran blue, eosin Y, etc.) (Table 1)[24].

348 On the other hand, the value of the kinetic constant, k , obtained with this model in
349 the present work is much higher than the specific substrate utilization rate coefficient

350 obtained in an ABR with three chambers (0.012 h^{-1}) processing molasses wastewater (9-
351 38 g COD/L) at OLRs of between 5-25 kg COD/m³ d (Table 1) [15]. By contrast, this
352 constant value is only slightly higher than the specific rate constant obtained in the
353 modelling of the anaerobic digestion of wastewater generated in orange juice production
354 (0.46 h^{-1}) using CSTR systems (Table 1) [25]. Finally, the value of k in the present
355 study is of the same order of magnitude as the maximum specific rate of substrate
356 consumption (0.70 h^{-1}) achieved in the methanogenesis from acetate using a periodic
357 ABR under increasing organic loading conditions (2700 to 10500 mg/L) (Table 1) [13].

358

359 3.2.2. *Validation of the CSTR in series model*

360 The proposed equations (2-4) were validated by comparing the theoretical curves
361 obtained with the corresponding experimental data of the fractional conversions for the
362 different operational conditions studied. Figure 5 shows the comparison of the
363 experimental fractional conversion data with the theoretical curves obtained using the
364 CSTR in series model for all the experiments carried out: those corresponding to HRTs
365 of 16 h and 8 h at a constant S_0 value of 3000 mg COD/L and those corresponding to
366 increasing influent substrate concentrations of 3000, 4500 and 6000 mg COD/L and a
367 constant HRT of 16 h. Figure 6 shows a comparison of the experimental data of
368 fractional conversion and theoretical data obtained with this model for all the
369 experiments carried out. As can be seen in both sets of experiments, deviations equal to
370 or lower than 10% between the experimental and simulated values of the fractional
371 conversion were obtained. However, a clear trend was observed in this model: the
372 theoretical fractional conversions obtained with the model were slightly higher than the
373 experimental values for almost all cases studied. Therefore, this simple model based on
374 a single parameter (such as the kinetic constant) allows for the adequate reproduction of

375 the fractional conversion values, which demonstrates that the kinetic parameter obtained
 376 represents approximately the activity of the different microorganisms involved in the
 377 anaerobic process. Table 2 summarizes the most significant statistical parameters (such
 378 as the non-linear regression coefficient (R), coefficient of determination (R^2), standard
 379 error of estimate, normality test (Shapiro-Wilk), W statistic and significance level)
 380 derived from the adjustment of the experimental data to this CSTR in series proposed
 381 model. The high values obtained for R and R^2 and the low values of the standard errors
 382 of estimates for the two HRTs studied (8 and 16 h) demonstrated the goodness of the
 383 model proposed.

384

385 3.2.3. Axial diffusion or Dispersion model

386 Assuming steady-state conditions in a bioreactor of length L for which a fluid
 387 flows with a constant rate u and the feed is axially mixed with a dispersion coefficient,
 388 D , and considering a first-order kinetics for substrate consumption, the following
 389 expression can be obtained [21]:

$$390 \quad (D/u \cdot L) d^2X/dz^2 - dX/dz + k \cdot \tau \cdot (1-X) = 0 \quad (5)$$

391 where X is the fractional conversion (per one), τ is the hydraulic retention time, z is the
 392 non dimensional length ($z = l/L$) and $(D/u \cdot L)$ is the dispersion coefficient and is equal to
 393 the inverse of the Peclet number.

394 Equation (5) can easily be converted into the following equation:

$$395 \quad X = 1 - [4 \cdot a \cdot \exp(u \cdot L / (2 \cdot D)) / [(1+a)^2 \cdot \exp(a \cdot u \cdot L / (2 \cdot D)) - (1-a)^2 \cdot \exp(-a \cdot u \cdot L / (2 \cdot D))]] \quad (6)$$

396 where $a = [1 + 4 \cdot k \cdot \tau \cdot (D / (u \cdot L))]^{0.5}$ and k is the kinetic constant of the process.

397 In conclusion, the dispersion model has two parameters which need to be calculated: the
 398 kinetic constant (k) and the dispersion coefficient (D).

399 According to the characteristics of this model and the experimental design used in
400 the present study, it is foreseeable that the dispersion model fits the experimental results
401 obtained better than the CSTR in series model. By solving equation (6) with the above-
402 mentioned Mathcad software, the following values for these parameters were obtained:
403 $k = 0.67 \pm 0.06 \text{ h}^{-1}$ and $D = 46$, therefore, the Peclet number, N , being equal to 0.02.

404 Taking into account the value of the dispersion coefficient obtained (46), the flow
405 pattern is intermediate between the plug-flow and completely stirred reactors (CSTR),
406 although it comes nearer to the plug-flow model. Consequently, the values of the kinetic
407 constant obtained with both models are quite similar.

408 A dispersion model was also found to be highly suitable for describing the
409 anaerobic digestion of municipal wastewater in a novel outside cycle reactor developed
410 based on the characteristics of an expanded granular sludge bed (EGSB) reactor [26].
411 The standard deviation of the simulated data (concentration of the effluent suspended
412 solids) was less than 6% (Table 1) [26]. The flow pattern and behaviour of an
413 acidogenic UASB reactor was also successfully simulated with the dispersion model.
414 The axial dispersion coefficient was identified as the most important factor in the
415 dispersion modelling of this reactor [27]. The axial dispersion model was also found to
416 be appropriate for studying the hydrodynamic pattern of a fluidised bed reactor [28] and
417 a rotating disc anaerobic reactor digesting acetic acid as substrate [29]. The feasibility of
418 the dispersion model simulating the process performance in anaerobic filters was also
419 reported in the literature [30].

420 Finally, similar small Peclet numbers (0.01-1.5) to those obtained in the present
421 study (0.02) were found in the deep-biofilm kinetics of substrate utilization during
422 acetate fermentation in anaerobic filters [31]. An axial dispersion model coupled with

423 deep biofilm kinetics can be better used to estimate the removal efficiency in this type
424 of reactors, as is also concluded in this work [31].

425

426 *3.2.4. Validation of the Dispersion model*

427 This newly proposed model was validated by comparing the simulated curves
428 obtained by means of equation (6) with the experimental values of the fractional
429 conversion for all the experiments carried out (Figure 7). The slight deviations obtained
430 (less than 8% in all cases) demonstrate the suitability of the proposed dispersion model
431 and suggest that this model describes the anaerobic digestion process of this wastewater
432 in the HABR more accurately than the CSTR in series model. All the statistical
433 parameters summarized in Table 2 indicate that, compared with the CSTR in series
434 model, the dispersion model slightly gives more accurate predictions of the reactor
435 performance than the CSTR in series model. Between the two flow hypotheses, plug-
436 flow appears to match the performance data more closely than the CSTR hypothesis
437 according to the statistical parameters evaluated.

438

439

440 **4. Conclusions**

441 The performance of a hybrid anaerobic baffled reactor treating molasses-based
442 synthetic wastewater was evaluated using two different kinetic models: a model of
443 CSTR in series and an axial diffusion or dispersion model. These models were assessed
444 and compared with the aim of simulating the organic matter removal or fractional
445 conversion under different operational conditions. The kinetic constant (k) obtained by
446 using the CSTR in series model was 0.6 h^{-1} , while the kinetic parameter of the
447 dispersion model and the dispersion coefficient (D) were 0.67 h^{-1} and 46, respectively.

448 The flow pattern and hydrodynamic behaviour observed in the hybrid reactor studied
449 was intermediate between plug-flow and CSTR in series systems, although the plug-
450 flow system was slightly predominant. The dispersion model allowed a slight better fit
451 of the experimental results of fractional conversions with deviations lower than 8%
452 between the experimental and theoretical values. On the basis of results obtained a study
453 using real molasses-based wastewater will be made in the future.

454

455 **Acknowledgements**

456

457 The authors gratefully acknowledge the financial support of the Water Research
458 Center of Greentech (Co. Ltd.), Shiraz, Iran. The authors also thank Dr. Anahita
459 Parsnejad for her help.

460

461

462 **References**

463

- 464 [1] Rao K.R., Srinivasan T., Venkateswarlu Ch. Mathematical and kinetic modelling
465 of biofilm reactor based on ant colony optimisation. *Process Biochem.*
466 2010;45:961-972.
- 467 [2] Sarti A., Pozzi E., Chinalia F.A., Ono A., Foresti E. Microbial processes and
468 bacterial populations associated to anaerobic treatment of sulfate-rich wastewater.
469 *Process Biochem.* 2010;45:164-170.
- 470 [3] Yu H.Q., Zhao Q.B., Tang Y. Anaerobic treatment of winery wastewater using
471 laboratory-scale multi- and single-fed filters at ambient temperatures. *Process*
472 *Biochem.* 2006;41:2477-2481.

- 473 [4] Chen S., Sun D., Chung J.S. Anaerobic treatment of highly concentrated aniline
474 wastewater using packed-bed biofilm reactor. *Process Biochem.* 2007;42:1666-
475 1670.
- 476 [5] Skiadas I.V., Gavala H.N., Lyberatos, G. Modelling of the periodic anaerobic
477 baffled reactor (PABR) based on the retaining factor concept. *Water Res.*
478 2000;34:3725-3736.
- 479 [6] Barber W.P., Stuckey D.C. The use of the anaerobic baffled reactor (ABR) for
480 wastewater treatment: a review. *Water Res.* 1999;33:1559-1578.
- 481 [7] Kuscu O.S., Sponza D.T. Treatment efficiencies of a sequential anaerobic baffled
482 reactor (ABR)/completely stirred tank reactor (CSTR) system at increasing p-
483 nitrophenol and COD loading rates. *Process Biochem.* 2006;41:1484-1492.
- 484 [8] Grover R., Marwaha S.S., Kennedy J.F. Studies on the use of an anaerobic baffled
485 reactor for the continuous anaerobic digestion of pulp and paper mill black
486 liquors. *Process Biochem.* 1999;34:653-657.
- 487 [9] Ghaniyari-Benis S., Borja R., Ali Monemian S., Goodarzi V. Anaerobic treatment
488 of synthetic medium-strength wastewater using a multistage biofilm reactor.
489 *Bioresour. Technol.* 2009;100:1740-1745.
- 490 [10] Galí A., Benabdallah T., Astals S., Mata-Alvarez J. Modified version of ADM1
491 model for agro-waste application. *Bioresour. Technol.* 2009;100:2783-2790.
- 492 [11] Martín-Santos M.A., Siles J., Chica A.F., Martín A. Modelling the anaerobic
493 digestion of wastewater derived from the pressing of orange peel produced in
494 orange juice manufacturing. *Bioresour. Technol.* 2010;101:3909-3916.
- 495 [12] Batstone D.J., Keller J., Newell R.B., Newland M. Modelling anaerobic
496 degradation of complex wastewater, I: model development. *Bioresour. Technol.*,
497 2000;75:67-74.

- 498 [13] Stamatelatou K., Lokshina L., Vavilin V., Lyberatos G. Performance of a glucose
499 fed periodic anaerobic baffled reactor under increasing organic loading conditions:
500 2. Model prediction. *Bioresour. Technol.*, 2003;88:137-142.
- 501 [14] Marin J., Kennedy K.J., Eskicioglu C., Hamoda M.F. Compartmental anaerobic
502 baffled reactor kinetic model for treatment of dilute aircraft de-icing fluid.
503 Proceedings of the Third IASTED International Conference on Environmental
504 Modelling and Simulation, EMS, 2007, Honolulu, Hawaii (USA), Ed. J. Wilson,
505 Acta Press, August 20-22, 2007, pp. 58-63.
- 506 [15] Xing J., Boopathy R., Tilche A. Model evaluation of hybrid anaerobic baffled
507 reactor treating molasses wastewater. *Biomass Bioenergy* 1991;5:267-274.
- 508 [16] Rajeshwari K.V., Balakrishnan M., Kansal A., Lata K., Kishore V.V.N. State of
509 the art of anaerobic digestion technology for industrial wastewater treatment.
510 *Renew. Sustain. Energy Rev.* 2000;4(2):135–156.
- 511 [17] Metcalf & Eddy, inc. *Wastewater engineering: Treatment, Disposal, and Reuse*,
512 4th. Ed., McGraw-Hill-New York, USA, 2003.
- 513 [18] Soto M., Veiga M.C., Mendez R., Lema J.M. Semi-micro COD determination
514 method for high-salinity wastewater. *Environ. Technol. Lett.* 1989;10(5):541–
515 548.
- 516 [19] American Public Health Association (APHA), American Water Works
517 Association, Water Environment Federation, APHA. *Standard methods for the
518 examination of water and wastewater*, 20th ed. Washington, DC; 1998.
- 519 [20] Björnsson L., Murto M., Mattiasson B. Evaluation of parameters for monitoring
520 an anaerobic co-digestion process. *Appl. Microbiol. Biotechnol.* 2000;54(6):844–
521 849.

- 522 [21] Levenspiel O. Modelling in chemical engineering. Chem. Eng. Sci.
523 2002;57:4691-4696.
- 524 [22] Danckwerts P.V. Continuous flow systems. Chem. Eng. Sci. 1953;2:1-18.
- 525 [23] Wehner J.F., Wilhelm R.H. Boundary conditions of flow reactor. Chem. Eng. Sci.
526 1995;50:3885-3888.
- 527 [24] De Nardi I.R., Zaiat M., Foresti E. Influence of the tracer characteristics on
528 hydrodynamic models of packed-bed bioreactors. Bioprocess Eng. 1999;21:469-
529 476.
- 530 [25] Siles J.A., Martín M.A., Martín A., Raposo F., Borja R. Anaerobic digestion of
531 wastewater derived from the pressing of orange peel generated in orange juice
532 production. J. Agric. Food Chem. 2007;55:1905-1914.
- 533 [26] Zhou X., Zhang Y., Zhang X., Jiang M. Simulation of sludge settling property in
534 a novel outside cycle anaerobic reactor. Huagong Xuebao/CIESC Journal
535 2009;60:738-743.
- 536 [27] Ren T.T., Mu Y., Yu H.Q., Harada H., Li Y.Y. Dispersion analysis of an
537 acidogenic UASB reactor. Chem. Eng. J. 2008;142:182-189.
- 538 [28] Otton V., Hihn J.Y., Béteau J.F., Delpech F., Chéruey A. Axial dispersion of liquid
539 in fluidised bed with external recycling: two dynamic modelling approaches with
540 a view to control. Biochem. Eng. J. 2000;4:129-136.
- 541 [29] Breithaupt T., Wiesmann U. Concentration profiles in rotating disc reactors: Their
542 mathematical model for the anaerobic digestion of acetic acid including an
543 experimental verification. Acta Hydrochim. Hydrobiol. 1998;16:288-295.
- 544 [30] Tseng S.K., Lin R.T., Liao K.L. Verification of dispersion model on anaerobic
545 reaction simulation. Water Sci. Technol. 1992;26:2377-2380.

546 [31] Huang J.S., Jih C.G. Deep-biofilm kinetics of substrate utilization in anaerobic
547 filters. Water Res. 1997;31:2309-2317.

548

549

550

551

552

553

554

555

556

557

558

559

560

561

562

563

564

565

566

567

568

569

570

571

572 **Table 1**

573 Comparison of the kinetic constants obtained in the present work with other values

574 reported in the literature

Substrate	Reactor type	Model used	Kinetic constant	Reference
Synthetic wastewater	Hybrid anaerobic baffled reactor	CSTR in series	0.60 h ⁻¹	Present study
Synthetic wastewater	Horizontal flow anaerobic immobilised sludge (HAIS) reactor	CSTR in series	0.45 h ⁻¹	[24]
Molasses	ABR	CSTR in series	0.012 h ⁻¹	[15]
Wastewater from orange juice production	CSTRs	CSTR in series	0.46 h ⁻¹	[25]
Acetate	Periodic ABR	CSTR in series	0.70 h ⁻¹	[13]
Synthetic wastewater	Hybrid anaerobic baffled reactor	Dispersion model	0.67 h ⁻¹	Present study
Municipal wastewater	Outside cycle reactor	Dispersion model	0.45 h ⁻¹	[26]

575

576

577

578

579

580

581

582

583

584

585

586 **Table 2**

587 Statistical parameters used in evaluating models performances

Parameter	CSTR in series model HRT = 8 h	CSTR in series model HRT = 16 h	Dispersion model
Non linear regression coefficient (R)	0.9995	0.9996	0.9998
Coefficient of determination (R^2)	0.9993	0.9994	0.9996
Standard error of estimate	0.0123	0.0138	0.0004
Normality test (Shapiro-Wilk)	Passed (P=0.3720)	Passed (P=0.5544)	Passed (P=0.0001)
W Statistic	0.8876	0.9231	0.6809
Significance level	0.0001	0.0001	0.0001

588

589

590

591

592

593

594

595

596

597

598

FIGURE CAPTIONS

599

600 **Figure 1.** Diagram of the hybrid anaerobic baffled reactor (HABR) and its baffles with
601 dimensions (cm).

602 **Figure 2.** Variation of the fractional conversion in the three compartments of the HABR
603 for the experiment corresponding to an HRT = 16 h.

604 **Figure 3.** Variation of the fractional conversion in the three compartments of the HABR
605 for the experiment corresponding to an HRT = 8 h.

606 **Figure 4.** Effect of the influent substrate concentration on the fractional conversion in
607 the three compartments of the HABR.

608 **Figure 5.** Variation of the experimental and theoretical values of the fractional
609 conversion (obtained with the CSTR in series model) with the hydraulic
610 retention time.

611 **Figure 6.** Comparison of the experimental and theoretical values of the fractional
612 conversion (obtained with the CSTR in series model) for all the experiments
613 carried out.

614 **Figure 7.** Comparison of the experimental and theoretical values of the fractional
615 conversion obtained with the dispersion model for all the experiments
616 carried out.

617

618

619

620

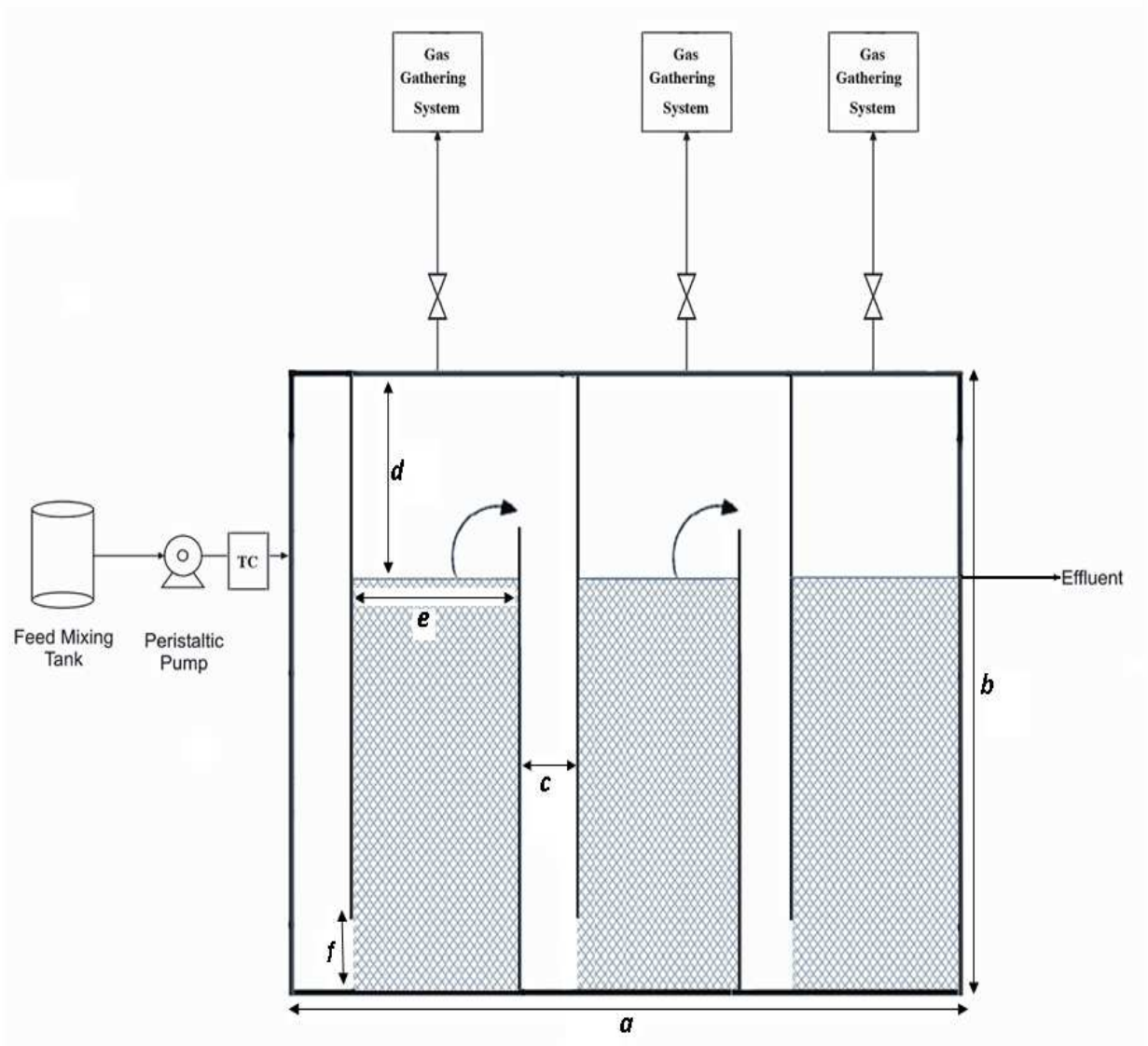


Figure 1

$a = 58 \text{ cm}; b = 44 \text{ cm}; c = 1.5 \text{ cm}; d = 6 \text{ cm}; e = 18 \text{ cm}; f = 2.5 \text{ cm}$

622
623
624
625
626
627
628
629
630
631
632
633
634
635
636
637
638
639
640

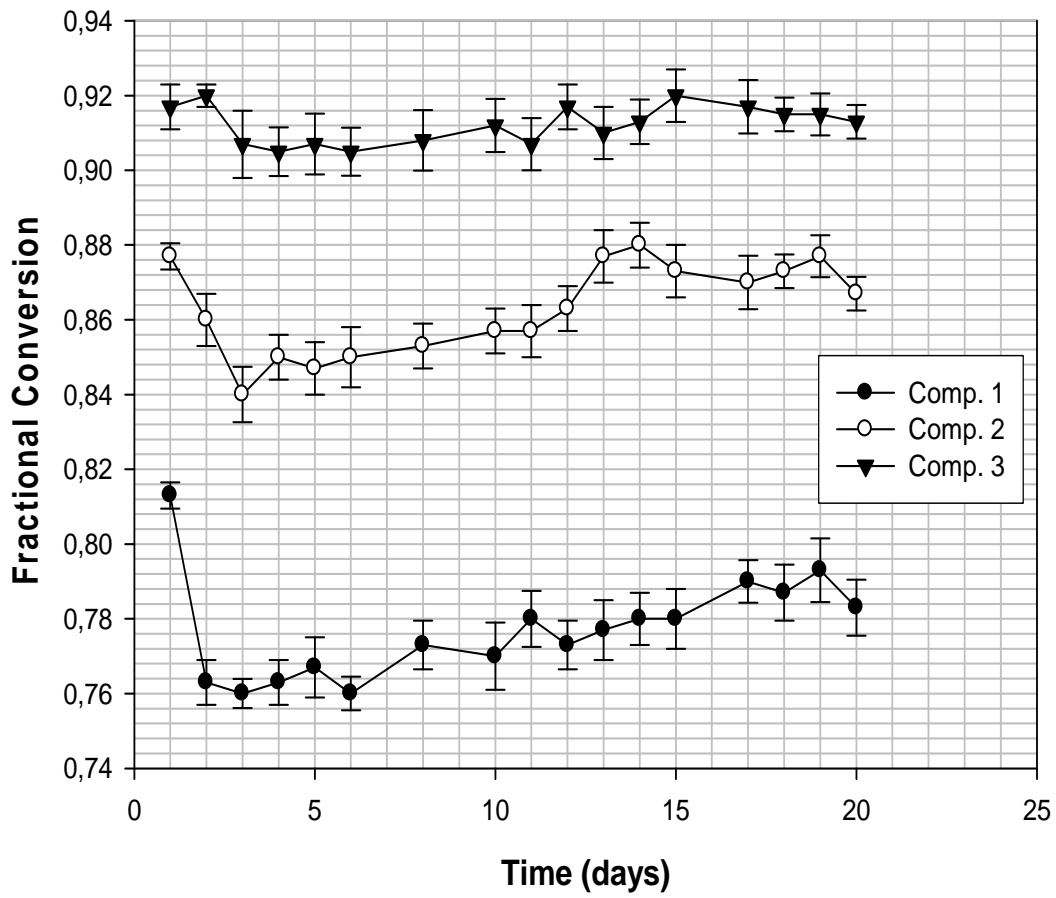


Figure 2

641
 642
 643
 644
 645
 646
 647
 648
 649
 650
 651
 652
 653
 654
 655
 656
 657
 658
 659
 660
 661
 662
 663
 664

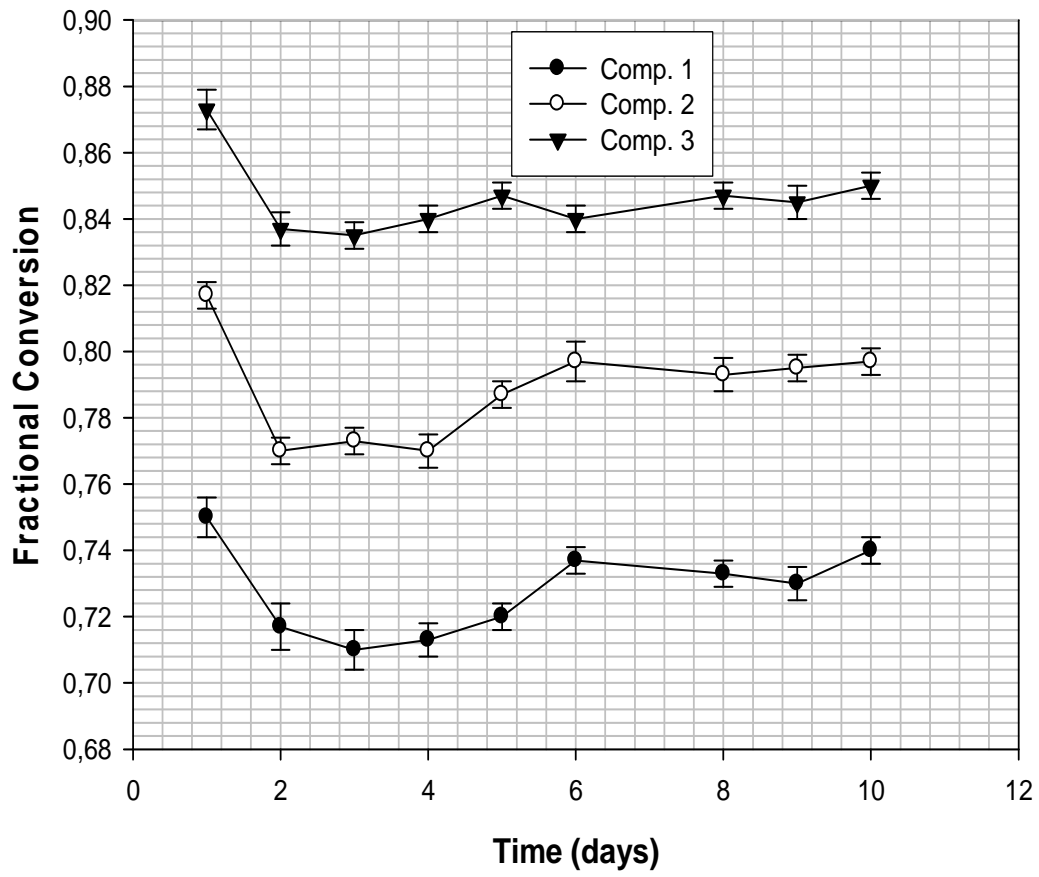


Figure 3

665
 666
 667
 668
 669
 670
 671
 672
 673
 674
 675
 676
 677
 678
 679
 680
 681
 682
 683
 684
 685
 686
 687
 688

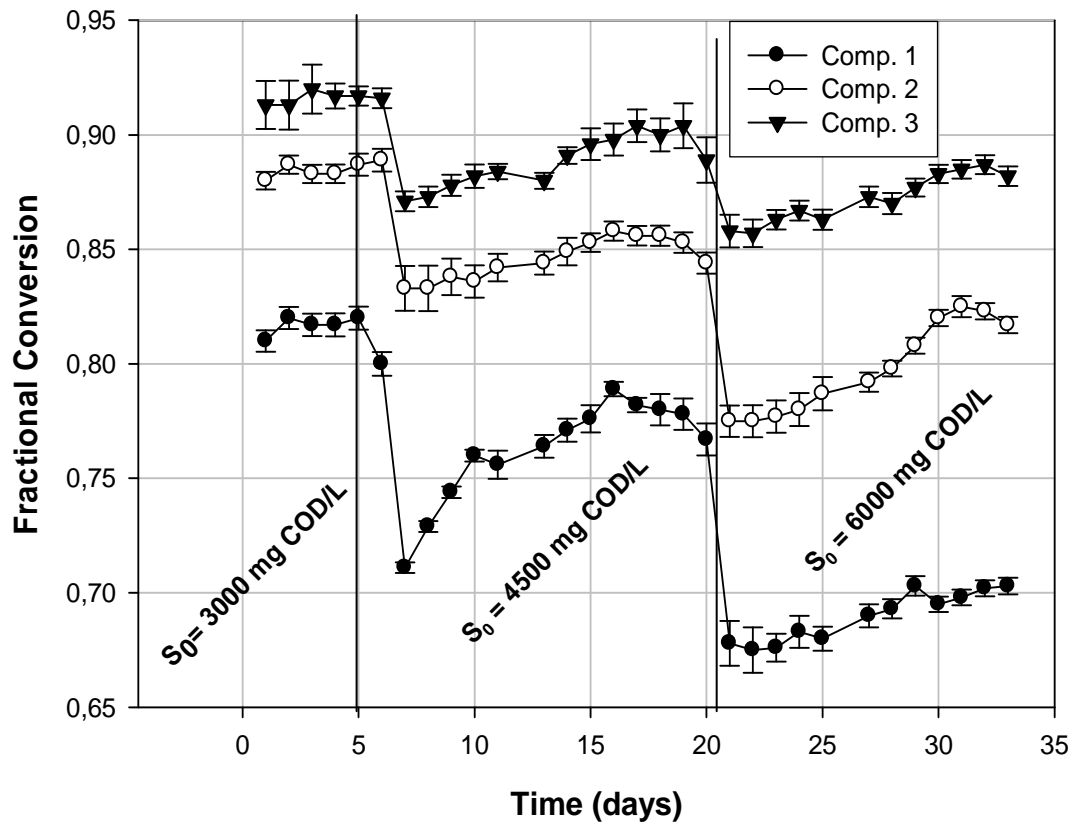


Figure 4

689
 690
 691
 692
 693
 694
 695
 696
 697
 698
 699
 700
 701
 702
 703
 704
 705
 706
 707

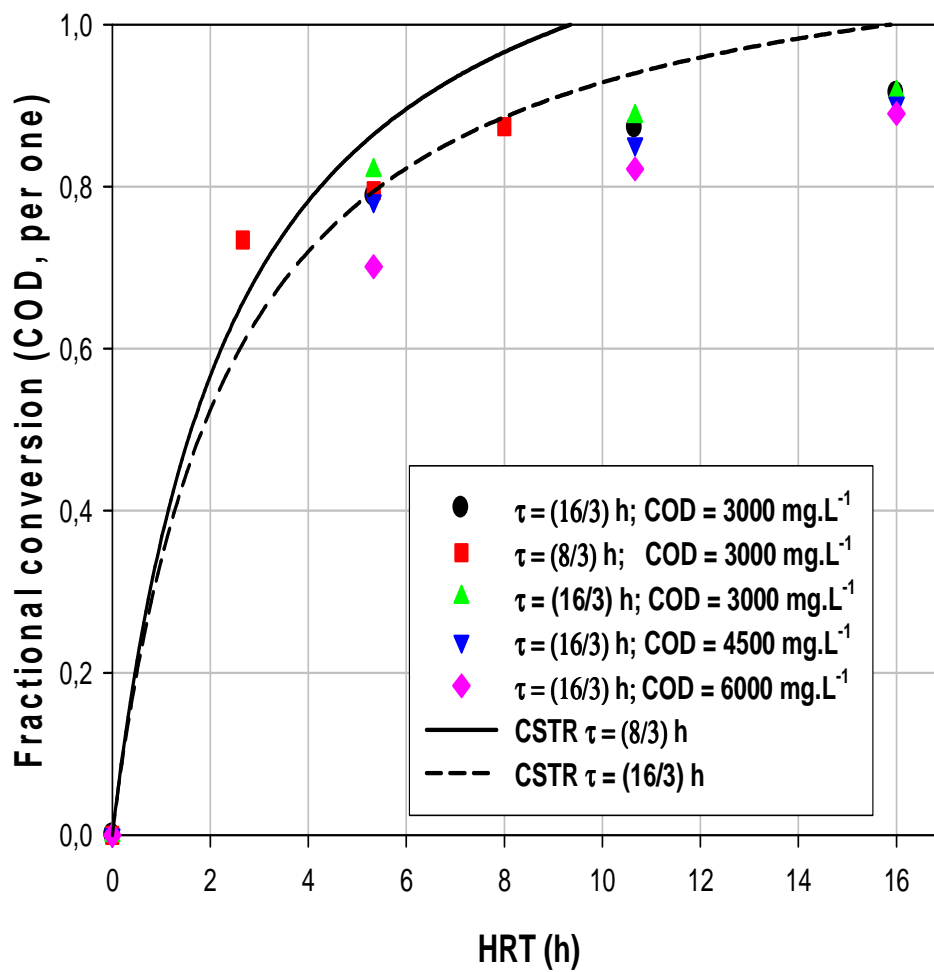
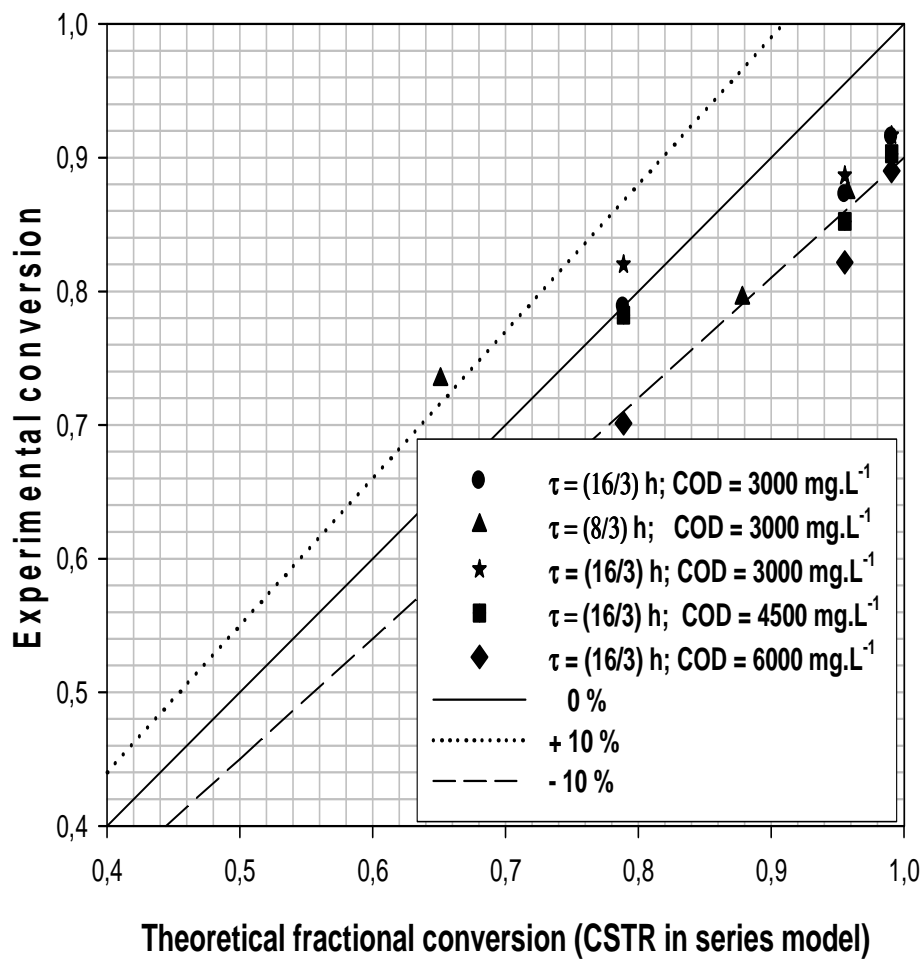


Figure 5

708
709
710
711
712
713
714
715
716
717
718
719
720
721
722
723
724
725
726
727
728
729



731
 732
 733
 734
 735
 736
 737
 738
 739
 740
 741
 742
 743
 744
 745
 746
 747
 748
 749
 750
 751

Figure 6

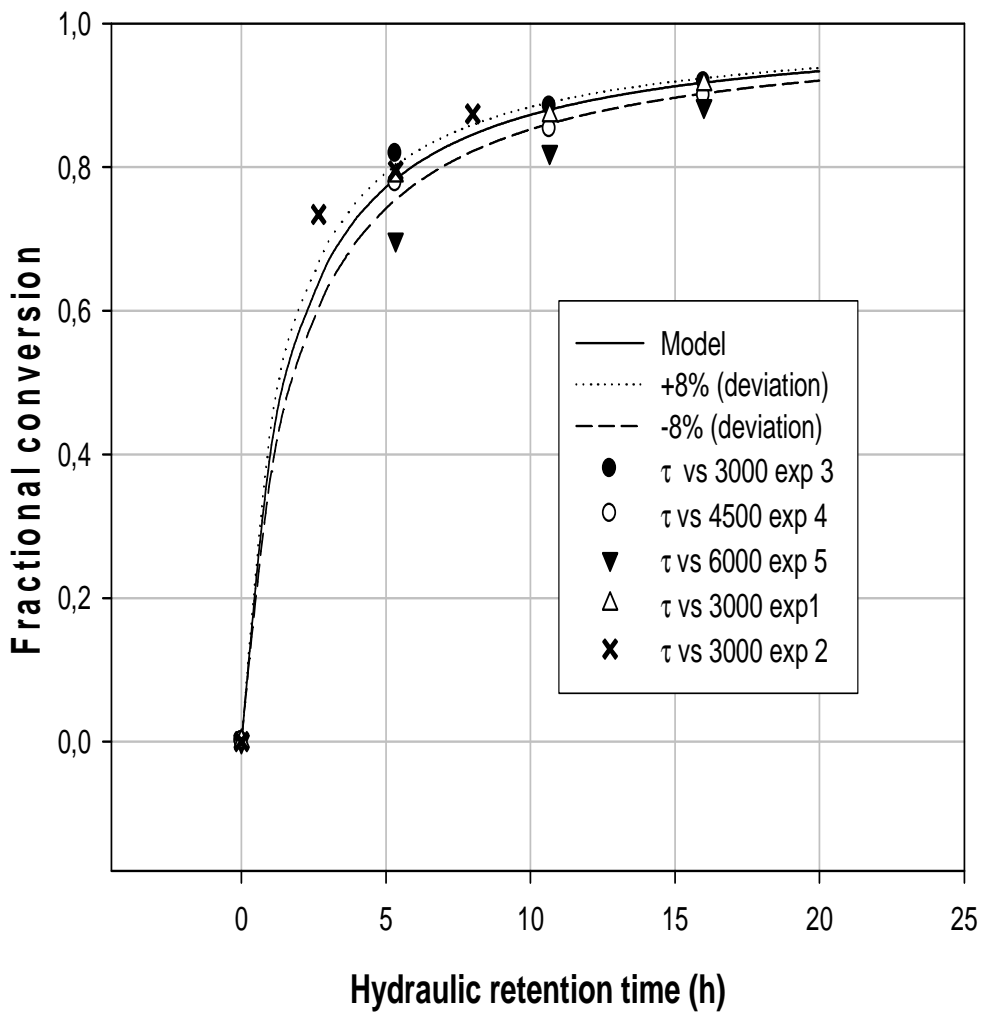


Figure 7

753

754

755

756

757

758

759